Biosensors and Bioelectronics 25 (2009) 282–287

Contents lists available at ScienceDirect

Biosensors and Bioelectronics

journal homepage: www.elsevier.com/locate/bios

A DNA biosensor based on the detection of doxorubicin-conjugated Ag nanoparticle labels using solid-state voltammetry

Boon Ping Ting, Jie Zhang, Zhiqiang Gao, Jackie Y. Ying*

Institute of Bioengineering and Nanotechnology, 31 Biopolis Way, The Nanos, Singapore 138669, Singapore

ARTICLE INFO

Article history:
Received 5 May 2009
Received in revised form 3 July 2009
Accepted 9 July 2009
Available online 17 July 2009

Keywords:
Flu virus H5N1
DNA biosensor
Electrochemistry
Silver nanoparticle labels
Solid-state voltammetry
Doxorubicin

ABSTRACT

This report describes an electrochemical biosensor for the detection of short DNA oligonucleotide of the avian flu virus H5N1 with sequence 5′-CCA AGC AAC AGA CTC AAA-3′. To fabricate this DNA biosensor, a gold (Au) electrode surface was modified with thiolated DNA probes with a sequence complementary to the target DNA. This modified Au electrode was incubated in a buffer solution containing the target DNA to form double-stranded DNA (ds-DNA) through hybridization. The ds-DNA on the electrode surface was then labeled with silver nanoparticles conjugated with a well-known DNA intercalator, doxorubicin. By performing cyclic voltammetry in an aqueous KCl solution (0.3 M), the silver nanoparticle labels were detected as a result of the highly characteristic solid-state Ag/AgCl redox process. The signal obtained was subsequently used to quantify the amount of DNA. A detection limit of 1 pM has been achieved with this new DNA biosensor.

1. Introduction

DNA biosensors have received significant attention due to their potential applications, including clinical diagnostics, forensic study and environmental monitoring (Ahmed et al., 2008; Kurian et al., 1999). Piezoelectric, optical and electrochemical techniques have been developed to achieve highly sensitive DNA detection (Teles and Fonseca, 2008; Sassolas et al., 2008; Drummond et al., 2003; Yang et al., 1997). The electrochemical approach is of particular interest, due to the following advantages: prompt detection, low cost, simplicity, high sensitivity and amenability to miniaturization on a chip (Ahmed et al., 2008; Gooding, 2002).

Advances in DNA biosensor have been realized with the development of surface DNA probe immobilization in conjunction with hybridization technique between complementary DNA sequences (Yang et al., 1997; Gooding, 2002). Several comprehensive studies for characterizing DNA probe immobilization have been reported (Peterlinz et al., 1997; Herne and Tarlov, 1997; Steel et al., 1998, 2000; Peterson et al., 2001). Since the concentration of the target DNA is extremely low, the sensitivity of DNA biosensor has to be very high in order to detect DNA directly. In addition to tuning the hybridization efficiency of the biosensor, different research groups have utilized signal amplification strategies to increase the sensitivity of the electrochemical biosensors (Wang et al., 2001; Patolsky et al., 1999; Alfonta et al., 2001; Wang et al., 2003a; Wang, 2005a; Kavanagh and Leech, 2006; Gao and Yang, 2006; Polsky et al., 2006; Hu et al., 2008; Bonanni et al., 2008). Two main signal amplification strategies have been employed: (a) labeling double-stranded DNA (ds-DNA) with either a reversible electron transfer mediator or a nanocatalyst that can mediate the electrolysis of a large quantity of substrate (Patolsky et al., 1999; Kavanagh and Leech, 2006; Gao and Yang, 2006; Polsky et al., 2006) and (b) increasing the loading of electroactive species, often by using metallic or semiconductor nanoparticle labels, e.g. Ag, Au, CdS, ZnS and PbS. In these cases, the large amount of metal atoms per nanoparticle label provides considerable signal amplification. Moreover, the use of different nanoparticles for different target analyte offers excellent multiplexing capabilities.

The loading of Au or Ag could be further increased after an enhancement step based on a seed mediated nucleation and growth mechanism (Wang et al., 2001, 2003b; Wang, 2005b; Katz et al., 2004; Luo et al., 2006; Guo and Wang, 2007; Castaneda et al., 2007). The latter signal amplification strategy is more relevant to the approach reported herein. In order to detect the nanoparticle labels electrochemically, the nanoparticles on the ds-DNA are oxidized with a strong oxidant, followed by stripping voltammetric detection of the dissolved metallic ions (Wang et al., 2001; Cai et al., 2002). To avoid this complicated pre-oxidation step, a specially designed magnetic electrode is used to collect the metallic nanoparticle–DNA–magnetic bead conjugates on the electrode surface. The metallic nanoparticles are detected by direct electrooxidation (Wang et al., 2002). Gao et al. (2008) reported a direct

* Corresponding author. Tel.: +65 6824 7100; fax: +65 6478 9020.
E-mail address: jyying@ibn.a-star.edu.sg (J.Y. Ying).

0956-5663/$ – see front matter © 2009 Elsevier B.V. All rights reserved.
doi:10.1016/j.bios.2009.07.005

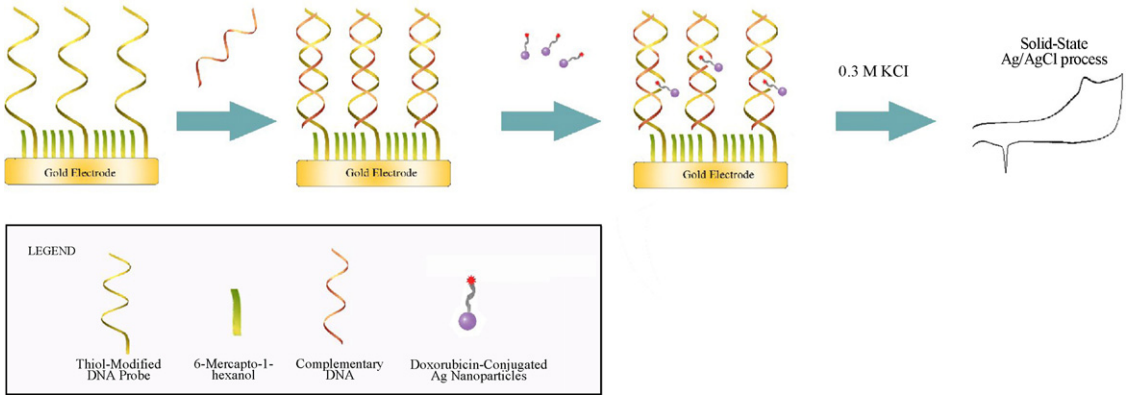

Fig. 1. Schematics of the biosensing strategy.

differential pulse voltammetric detection of Ag nanoparticle labels. A detection limit of 1 nM of DNA was achieved, which was much higher than the values of 1 fM–1 pM attained by the other electrochemical DNA biosensors with nanoparticles as labels. Gao et al. (2008) managed to achieve a much lower detection limit of 10 fM when Ag-loaded carbon nanotubes were used as labels to increase the loading of Ag nanoparticles.

We have recently reported a simple strategy involving the labeling of the ds-DNA with Ag nanoparticles, followed by the detection of a highly characteristic solid-state Ag/AgCl process (Zhang et al., 2009). Neutral PNA probes were employed in that study. After hybridization with the target DNA, the electrode surface became negatively charged, and thus could be labeled with positively charged Ag nanoparticles. This electrode was then placed in an aqueous KCl solution. The amount of DNA was detected via the solid-state Ag/AgCl process. A detection limit of 10 fM has been achieved. However, PNA is associated with high costs, and a much cheaper DNA-based probe would be preferred. This implies that the labeling strategy based on electrostatic attraction would need to be replaced by another mechanism for quantifying the hybridized DNA.

Chemical reagents, known as intercalators, can bind strongly to ds-DNA through intercalation. Electroactive intercalators have been widely used in the development of ultrasensitive electrochemical DNA biosensors as both a hybridization indicator and an electron transfer mediator for the electrolysis of a large concentration of substrates for the purpose of signal amplification (Wong and Gooding, 2006; Kara et al., 2002; Mascini et al., 2001; He et al., 2005). Doxorubicin is one of the many intercalators that has been extensively studied (Yang and Wang, 1999). It has a high binding constant with ds-DNA ($\sim 10^6\ M^{-1}$) (Yang et al., 1998; Messori et al., 2001; Patolsky et al., 2002; Zeman et al., 1998). Herein we report the application of doxorubicin-conjugated Ag nanoparticles as the labels for DNA sensing. The Ag nanoparticles are then electrochemically detected via the highly characteristic solid-state Ag/AgCl process (Fig. 1).

2. Experimental

2.1. Materials and reagents

3′ thiolated oligonucleotide probe (sequence: 5′-TTT GAG TCT GTT GCT TGG AAA AAA-3′), target oligonucleotide (sequence: 5′-CCA AGC AAC AGA CTC AAA-3′), 1 M of tris (hydroxymethyl)aminomethane (TRIS) buffer (pH 7.0), 20× saline sodium citrate (SSC) buffer solution (1× SSC contained 0.15 M of sodium chloride and 0.015 M of sodium citrate), and 10% (w/v) sodium dodecyl sulfate (SDS) solution were obtained from 1st Base Pte. Ltd. O,O′-bis[2-(N-succinimidyl-succinylamino)-ethyl] polyethylene glycol 3,000 (NHS-PEG-NHS), 6-mercapto-1-hexanol (MCH), sodium borohydride ($NaBH_4$), potassium phosphate monobasic (KH_2PO_4), sodium chloride (NaCl), sodium hydroxide (NaOH), ethylenediaminetetraacetic acid (EDTA), silver nitrate ($AgNO_3$) and doxorubicin were obtained from Sigma–Aldrich. Reagents used for the synthesis of the polymer capping agent of the Ag nanoparticles, including pentaethylenehexamine (technical grade), methyl-3-mercaptopropionate, tris(2-aminoethyl)amine (96%), and epichlorohydrin, were obtained from Sigma–Aldrich. PD-10 disposable desalting columns were obtained from GE healthcare. Nanopure water (resistivity > 18 kΩ cm) was used.

2.2. Apparatus

Cyclic voltammetry was performed with a CHI 400 electrochemical analyzer (CH Instruments, Austin, Texas). A conventional 3-electrode system was employed. A 2 mm-diameter gold electrode (CH Instruments), a platinum wire and a Ag/AgCl (3 M KCl) electrode (CH Instruments) were used as the working electrode, counter electrode and reference electrode, respectively. Fluorescence and absorption spectra were obtained with a Fluorolog®-3 spectrofluorometer (Jobin Yvon Inc., New Jersey) and an Agilent 8453 UV–vis spectrometer, respectively. TEM experiments were performed on a JEOL JEM-3010 electron microscope (200 kV). Centrifugation was done using an Allegra 64R Centrifuge (Beckman Coulter, California).

2.3. Synthesis and conjugation of Ag nanoparticles

The capping agent used for the synthesis of the Ag nanoparticles was a low molecular weight polymer that contained both disulfide and primary amine. The synthesis of this polymer has been described in detail in our previous paper (Ting et al., 2009). The Ag nanoparticles were prepared by the chemical reduction of Ag^+ ions in the presence of the capping agent. Briefly, 1 mM of $AgNO_3$ and 0.5 mg/ml of polymer were dissolved in 200 ml of water, and stirred for 10 min. 15 mg of $NaBH_4$ dissolved in 2 ml of water were added dropwise, resulting in a dark brown solution. The solution was then concentrated to 10 ml through evaporation. The nanoparticles were separated from the reaction mixture by precipitating in a water/acetone mixture and centrifugation at 21,000 rpm. The supernatant was discarded, while the precipitate was re-dissolved in water. This procedure was repeated twice to ensure the high purity of the final product. The synthesized Ag nanoparticles were re-dissolved in 10 ml of water as a stock solution for further application. They displayed an absorption band at 404 nm, which corresponded to the characteristic surface plasma resonance band of Ag nanoparticles. TEM

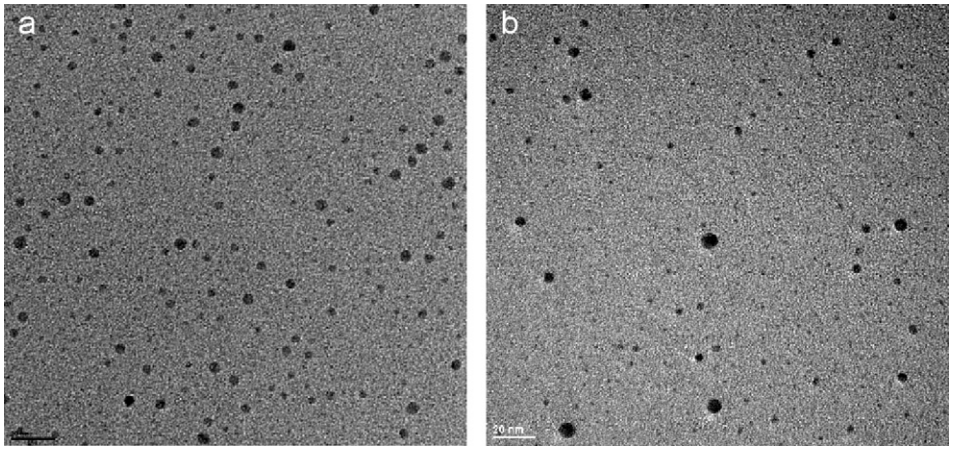

Fig. 2. TEM images of Ag nanoparticles (a) before and (b) after conjugation with doxorubicin. Scale bar = 20 nm.

image showed that the Ag nanoparticles were ~5 nm in diameter (Fig. 2a).

The Ag nanoparticles were conjugated with doxorubicin through their primary amines by utilizing the NHS-PEG-NHS bifunctional linker. Firstly, 0.850 mg of Ag nanoparticles was diluted in 1 ml of borate buffer (pH 7.5), and mixed with an excessive amount of NHS-PEG-NHS (10 mg dissolved in 100 μl of dimethyl sulfoxide (DMSO)), so that statistically only one NHS from NHS-PEG-NHS could react with a primary amine on the Ag nanoparticle surface. Cross-linking and aggregation could thus be minimized. This solution was incubated for 5–15 min before the NHS-PEG-NHS-conjugated nanoparticles were passed through the Sephadex column to remove excess NHS-PEG-NHS. Incubation time was varied to control the amount of NHS-PEG-NHS per Ag nanoparticle, so as to manipulate the loading of doxorubicin per Ag nanoparticle. The NHS-PEG-NHS-activated Ag particles were immediately mixed with 1 ml of 5 mM of doxorubicin, and incubated for 2 h under shaking. Next, 100 μl of 1 M of tris(hydroxymethyl) aminomethane (TRIS) buffer (pH 7.0) were added to block any unreacted NHS groups. The conjugated nanoparticles were passed through the Sephadex columns twice to completely remove unbound doxorubicin. The successful conjugation between doxorubicin and Ag nanoparticles was confirmed by the doxorubicin fluorescence at ~590 nm (Karukstis et al., 1998) exhibited by the conjugated Ag nanoparticle solution. The fluorescence peak of doxorubicin was also used to quantify the doxorubicin loading on the Ag nanoparticles. TEM image showed that the Ag nanoparticles remained unchanged in size after conjugation (Fig. 2b). The doxorubicin-conjugated Ag nanoparticles were stored in the dark at 4 °C.

2.4. Electrode modification, DNA hybridization and detection

The gold electrode modification and DNA hybridization detection procedures were illustrated in Fig. 1. The gold electrode was polished with a 0.3 μm alumina slurry on a microcloth pad (Buehler, Illinois) for 3–5 min. The electrode was next sonicated in water for a few minutes. The electrode was then electrochemically cleaned in 0.5 M of H_2SO_4 (by cycling between −0.2 and 0.85 V versus a Pt quasi-reference electrode for 60 cycles), to ensure a complete removal of contaminants on the electrode surface. Immediately after cleaning, the electrode was rinsed with water, and incubated with 1 μM of thiolated oligonucleotide probe in 1 M of KH_2PO_4 (pH 4.5) for 10 min. The electrode was then rinsed with water. To ensure a high hybridization efficiency (Herne and Tarlov, 1997), the electrode was exposed to 1 mM of MCH for 1 h, followed by washing with water. This DNA/MCH-immobilized gold electrode was placed in contact with the target DNA dissolved in 10 mM of Tris–HCl/1.0 mM of EDTA/1.0 M of NaCl for hybridization at room temperature to form the ds-DNA. After 1 h, the electrode was rinsed with 10 mM of Tris–HCl/0.15 M of NaCl (pH 8.8), followed by 2 × SSC buffer/0.2% of SDS. The electrode was rinsed again with 10 mM of Tris–HCl/0.15 M of NaCl (pH 8.8). This electrode was then exposed to the doxorubicin-conjugated Ag nanoparticle solution (pH 7.0, dissolved in 10 mM of Tris buffer solution) for 20 min, allowing for doxorubicin to be intercalated in the ds-DNA. The electrode was washed carefully with 10 mM of Tris–HCl/0.15 M of NaCl (pH 8.8) and with 0.1 M of KCl consecutively before performing cyclic voltammetric studies at a scan rate of 0.1 V s^{-1}.

3. Results and discussion

3.1. Detection of Ag nanoparticle labels using solid-state voltammetry

Cyclic voltammetric measurements were first conducted in 0.3 M of KNO_3. However, no obvious signals related to Ag oxidation/reduction were observed from 0 to 1.2 V, which was consistent with our previous finding (Zhang et al., 2009), presumably due to the strong protection of the Ag nanoparticles by the capping agent and the fact that linear sweep stripping voltammetry was less sensitive as compared to the solid-state voltammetry for Ag detection (Zhang et al., 2009). In contrast, when the voltammetric experiments were conducted in 0.3 M of KCl, two well-defined current peaks were observed (see Fig. 3). In the anodic potential sweep, a very sluggish process was observed between 0.4 and 0.7 V, corresponding to the oxidation of Ag nanoparticles. Due to the formation of AgCl, the oxidation of Ag nanoparticles became much easier. In the presence of Cl^-, the electrogenerated Ag^+ formed insoluble AgCl on the electrode surface. In the reverse cathodic potential scan, AgCl was reduced to Ag, and Cl^- was simultaneously released into the solution. A sharp peak with a peak width at half height of ~18 mV was observed at 0.122 V. This peak width was much narrower than those associated with any other voltammetric processes (Bard and Faulkner, 2001), as was typical for a solid-state electrochemical process (Bond et al., 1998; Scholz and Meyer, 1989). The two solid-state processes mentioned above were represented by Eqs. (1) and (2) in the simplest forms,

$$\text{Ag nanoparticle (s)} + n\text{Cl}^- \text{(solution)} \rightarrow n\text{AgCl (s)} + ne^- \quad (1)$$

$$\text{AgCl (s)} + e^- \Leftrightarrow \text{Ag (s)} + \text{Cl}^- \text{(solution)} \quad (2)$$

The concentration of the target DNA determined the amount of nanoparticle labels bound to the hybridized ds-DNA, which in turn established the peak magnitude, allowing for the quantifi-

cation of the target DNA. It was found that process (2) produced a much larger peak current. Moreover, the signal produced from this process was easily distinguished from the background signal, which made the background subtraction straightforward. Therefore, the well-defined and sharp peak generated by process (2) was employed for DNA sensing.

The solid-state Ag/AgCl process is advantageous because it is simple and highly characteristic. The solid-state Ag/AgCl process described herein possesses distinct voltammetric features that are different from those in the background processes. This is in stark contrast to the other types of electrochemical processes whereby a small signal may not be easily differentiated from the background. The detection of Ag nanoparticles using the solid-state Ag/AgCl process is also anticipated to have higher sensitivity as compared to the conventional stripping voltammetric methods. This is attributed to the very narrow peak associated with the Ag/AgCl process. The area underneath this peak is proportional to the charge consumed. For a given amount of electroactive species involved, the solid-state electrochemical process is expected to have a much higher peak current as compared to the other types of processes.

3.2. Effect of KCl concentration

It is expected from Eq. (2) that the characteristics of the solid-state Ag/AgCl process are affected by the concentration of Cl^-. To investigate the effect of KCl, especially on the peak width and peak height of the solid-state Ag/AgCl process, voltammetric experiments were conducted on solutions containing different amounts of KCl (0.08–0.5 M). The average values of the peak width at half height and the peak current for six parallel experiments conducted for the measurement of 10 nM of target DNA were summarized in Fig. 4. The relative standard deviation (RSD) for each of these data points was ~10–15%. The results indicated that the peak width at half height became smaller at a higher KCl concentration; the maximum peak current was also significantly reduced when the KCl concentration was ≥0.4 M of KCl. Therefore, 0.3 M of KCl was chosen for this study.

3.3. Effect of the surface density of immobilized DNA probes on the sensitivity of the biosensor

The surface density of immobilized DNA probes has a profound effect on the hybridization efficiency with the target DNA (Herne and Tarlov, 1997; Peterson et al., 2001). When the probe density

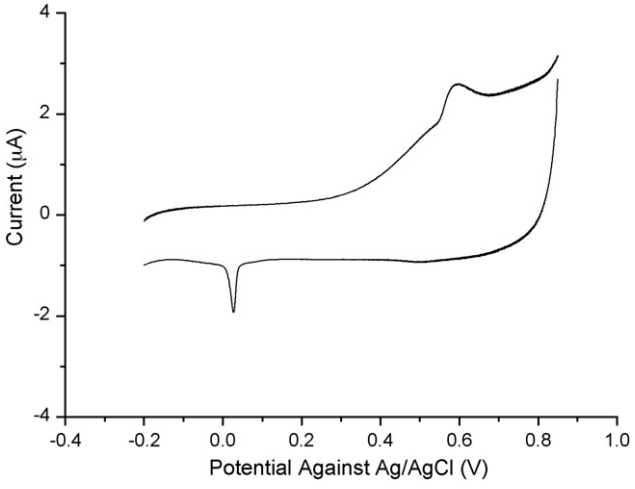

Fig. 3. Typical voltammetric response of the DNA biosensor in 0.3 M of KCl after hybridization with 1 nM of target DNA.

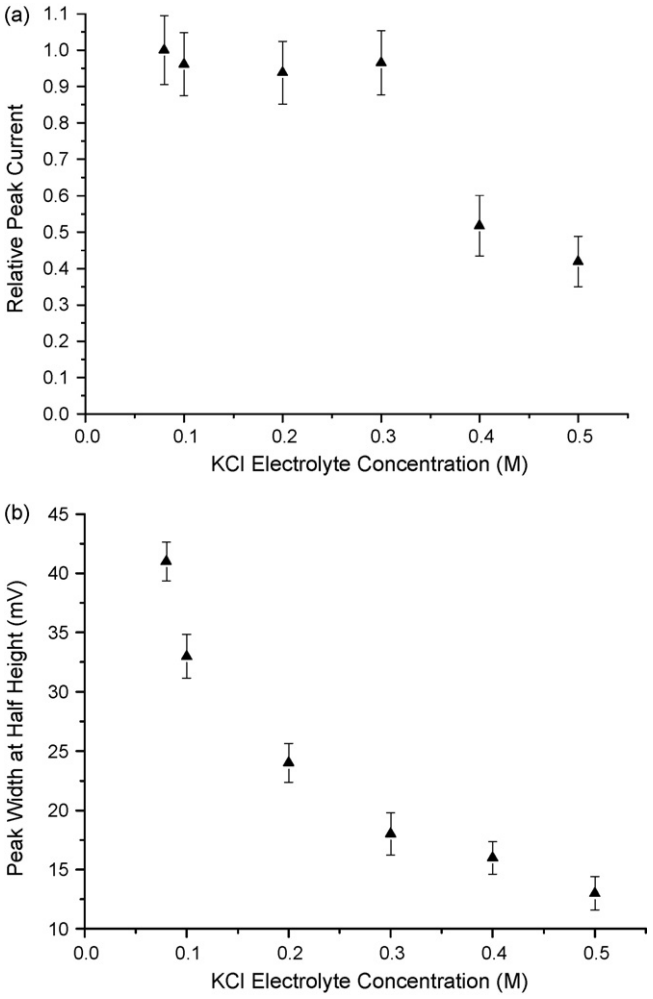

Fig. 4. Effect of KCl concentration on the (a) peak current normalized by peak height obtained with 0.08 M of KCl, and (b) peak width at half height.

is too high, hybridization efficiency is reduced. Based on the study conducted by Herne and Tarlov (1997), the greatest hybridization efficiency is achieved when the electrode surface is exposed to 1 μM of thiolated DNA for 120 min, followed by 1 mM of MCH for 60 min. The surface density of the probes was $\sim 5.2 \times 10^{12}$ molecules/cm^2 under these conditions. In this study, the surface density of the DNA probes could also affect the efficiency of labeling since the Ag nanoparticles have a typical size of 5 nm, instead of Ångstroms as in the case of a molecule. The labeling efficiency was expected to decrease when the probe density was too high due to the steric hindrance effect. Therefore, experiments were conducted to examine the effect of probe density on the sensitivity of the biosensor. The probe density was varied by changing the immobilization period, while keeping the duration for the MCH step constant (at 60 min). The results suggested that the highest sensitivity was obtained when a clean Au electrode was incubated with thiolated probe DNA for 10 min.

3.4. The effect of doxorubicin loading on the sensitivity

As mentioned earlier, the sensitivity of biosensor depends on the labeling efficiency with the target DNA. The labeling method for this study involves the intercalation of doxorubicin with the ds-DNA. Therefore, experiments were also conducted to examine the effect of doxorubicin loading per nanoparticle on the sensitivity of the DNA biosensor. Our results indicated that the highest sensitiv-

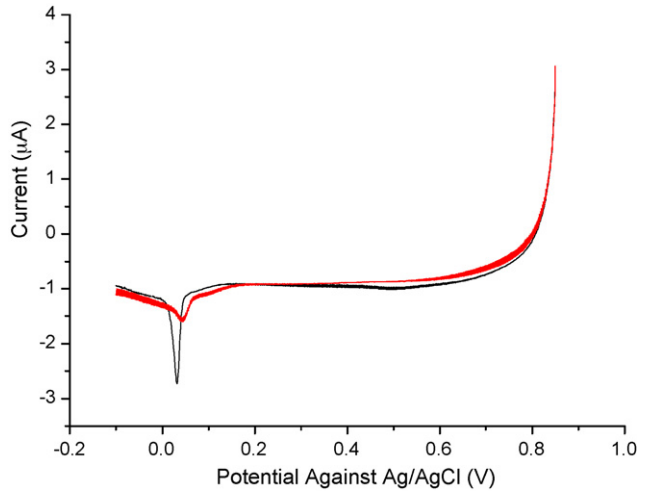

Fig. 5. Comparison of voltammetric results measured in 0.3 M of KCl when a doxorubicin loading per Ag nanoparticle of (▬) ~17 and (▬) ~1 was used in the labeling process. Electrodes with the optimal probe density were incubated in 50 μl of 10 nM of the target DNA for hybridization before labeling.

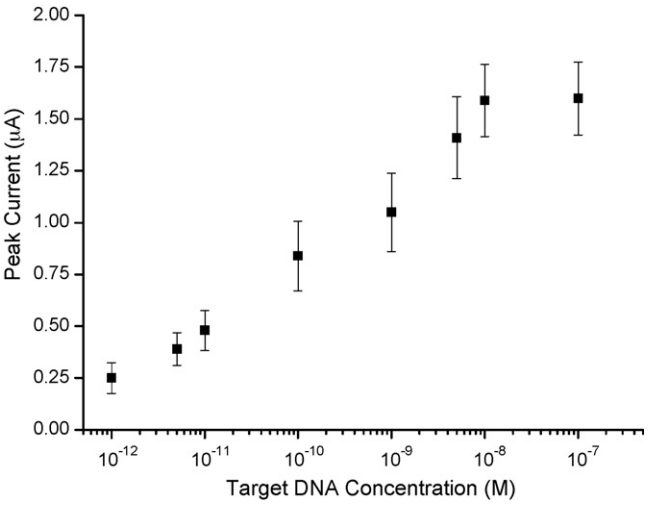

Fig. 6. Calibration curve of the DNA biosensor obtained under optimal conditions. The error bars indicate one standard deviation from the average of the peak current for each concentration.

ity was achieved when the doxorubicin loading per nanoparticle was ~1. When the doxorubicin loading per nanoparticle was much higher than 1, the sensitivity would decrease. As shown in Fig. 5, at a loading of ~17 doxorubicin per Ag nanoparticle, intercalation was highly unfavourable. This was likely due to the fact that having an overwhelming amount of doxorubicin on the Ag nanoparticles presented a steric hindrance to intercalation with the ds-DNA on the electrode.

3.5. Calibration curve for DNA detection

Under the optimal conditions, this biosensor has a good response to DNA over a wide range of concentrations. Fig. 6 shows a calibration curve, and the error bars were taken as one standard deviation associated with each measurement obtained from six parallel experiments. A RSD of up to ~30% was associated with the measurements when the concentration of DNA was 1 pM. This RSD could be as small as ~10% when the DNA concentration was higher than 10 nM. As a result of the adsorption isotherm, the peak current increased linearly with the logarithm of the target DNA concentration as the DNA concentration was increased from 1 pM to 10 nM. The lowest detectable concentration of 1 pM was taken as the detection limit. This was comparable to those obtained by the other researchers when Ag nanoparticles were used as labels for the electrochemical detection of DNA without using a Ag enhancement step (Cai et al., 2002), but less sensitive compared to our previous study where neutral PNA was used as capture probe (Zhang et al., 2009). The peak current approached a plateau when the target DNA concentration was ≥10 nM. Controlled experiments with non-complementary DNA showed negligible response comparable to that of a blank solution.

4. Conclusions

In summary, we have successfully synthesized doxorubicin-conjugated Ag nanoparticles as labels in the electrochemical detection of DNA using the thiolated DNA probe modified gold electrode. These Ag nanoparticle labels were detected through the highly characteristic solid-state Ag/AgCl redox process. The derived ultrasensitive DNA biosensor operated in a simple and yet effective manner to achieve a low detection limit of 1 pM.

Acknowledgments

This work was funded by the Institute of Bioengineering and Nanotechnology (Biomedical Research Council, Agency for Science, Technology and Research, Singapore). The authors thank Dr. Majad Khan for the synthesis of the low molecular weight polymer, and Dr. Alex W. H. Lin for helpful discussions.

References

Ahmed, M.U., Hossain, M.M., Tamiya, E., 2008. Electroanalysis 20, 616–626.
Alfonta, L., Singh, A.K., Willner, I., 2001. Anal. Chem. 73, 91–102.
Bard, A.J., Faulkner, L.R., 2001. Electrochemical Methods: Fundamentals and Applications, 2nd ed. John Wiley & Sons, New York.
Bonanni, A., Esplandiu, M.J., del Valle, M., 2008. Electrochim. Acta 53, 4022–4029.
Bond, A.M., Fletcher, S., Symons, P.G., 1998. Analyst 123, 1891–1904.
Cai, H., Xu, Y., Zhu, N.N., He, P.G., Fang, Y.Z., 2002. Analyst 127, 803–808.
Castaneda, M.T., Alegret, S., Merkoci, A., 2007. Electroanalysis 19, 743–753.
Drummond, T.G., Hill, M.G., Barton, J.K., 2003. Nat. Biotechnol. 21, 1192–1199.
Gao, M., Qi, H., Gao, Q., Zhang, C., 2008. Electroanalysis 20, 123–130.
Gao, Z.Q., Yang, Z.C., 2006. Anal. Chem. 78, 1470–1477.
Gooding, J.J., 2002. Electroanalysis 14, 1149–1156.
Guo, S.J., Wang, E.K., 2007. Anal. Chim. Acta 598, 181–192.
He, P.A., Xu, Y., Fang, Y.Z., 2005. Anal. Lett. 38, 2597–2623.
Herne, T.M., Tarlov, M.J., 1997. J. Am. Chem. Soc. 119, 8916–8920.
Hu, K.C., Lan, D.X., Li, X.M., Zhang, S.S., 2008. Anal. Chem. 80, 9124–9130.
Kara, P., Kerman, K., Ozkan, D., Meric, B., Erdem, A., Ozkan, Z., Ozsoz, M., 2002. Electrochem. Commun. 4, 705–709.
Karukstis, K.K., Thompson, E.H.Z., Whiles, J.A., Rosenfeld, R.J., 1998. Biophys. Chem. 73, 249–263.
Katz, E., Willner, I., Wang, J., 2004. Electroanalysis 16, 19–44.
Kavanagh, P., Leech, D., 2006. Anal. Chem. 78, 2710–2716.
Kurian, K.M., Watson, C.J., Wyllie, A.H., 1999. J. Pathol. 187, 267–271.
Luo, X.L., Morrin, A., Killard, A.J., Smyth, M.R., 2006. Electroanalysis 18, 319–326.
Mascini, M., Palchetti, I., Marrazza, G., 2001. Fresenius J. Anal. Chem. 369, 15–22.
Messori, L., Temperini, C., Piccioli, F., Animati, F., Di Bugno, C., Orioli, P., 2001. Bioorg. Med. Chem. 9, 1815–1825.
Patolsky, F., Katz, E., Bardea, A., Willner, I., 1999. Langmuir 15, 3703–3706.
Patolsky, F., Katz, E., Willner, I., 2002. Angew. Chem. Int. Ed. 41, 3398–3402.
Peterlinz, K.A., Georgiadis, R.M., Herne, T.M., Tarlov, M.J., 1997. J. Am. Chem. Soc. 119, 3401–3402.
Peterson, A.W., Heaton, R.J., Georgiadis, R.M., 2001. Nucleic Acids Res. 29, 5163–5168.
Polsky, R., Gill, R., Kagnovsky, L., Willner, I., 2006. Anal. Chem. 78, 2268–2271.
Sassolas, A., Leca-Bouvier, B.D., Blum, L.J., 2008. Chem. Rev. 108, 109–139.
Scholz, F., Meyer, B., 1989. In: Bard, A.J. (Ed.), Electroanalytical Chemistry, vol. 15. Marcel Dekker, New York, p. 1.
Steel, A.B., Herne, T.M., Tarlov, M.J., 1998. Anal. Chem. 70, 4670–4677.
Steel, A.B., Levicky, R.L., Herne, T.M., Tarlov, M.J., 2000. Biophys. J. 79, 975–981.
Teles, F.R.R., Fonseca, L.P., 2008. Talanta 77, 606–623.
Ting, B.P., Zhang, J., Khan, M., Yang, Y.Y., Ying, J.Y., 2009. Chem. Commun, in press.
Wang, J., 2005a. Electroanalysis 17, 7–14.
Wang, J., 2005b. Electrochemistry of Nucleic Acids and Proteins, vol. 1. Elsevier, Amsterdam, pp. 369–384.

Wang, J., Li, J.H., Baca, A.J., Hu, J.B., Zhou, F.M., Yan, W., Pang, D.W., 2003a. Anal. Chem. 75, 3941–3945.
Wang, J., Rincon, O., Polsky, R., Dominguez, E., 2003b. Electrochem. Commun. 5, 83–86.
Wang, J., Xu, D.K., Kawde, A.N., Polsky, R., 2001. Anal. Chem. 73, 5576–5581.
Wang, J., Xu, D.K., Polsky, R., 2002. J. Am. Chem. Soc. 124, 4208–4209.
Wong, E.L.S., Gooding, J.J., 2006. Anal. Chem. 78, 2138–2144.
Yang, M.S., McGovern, M.E., Thompson, M., 1997. Anal. Chim. Acta 346, 259–275.
Yang, M.S., Yau, H.C.M., Chan, H.L., 1998. Langmuir 14, 6121–6129.
Yang, X.L., Wang, A.H.J., 1999. Pharmacol. Ther. 83, 181–215.
Zeman, S.M., Phillips, D.R., Crothers, D.M., 1998. Proc. Natl. Acad. Sci. U.S.A. 95, 11561–11565.
Zhang, J., Ting, B.P., Jana, N.R., Gao, Z.Q., Ying, J.Y., 2009. Small 5, 1414–1417.